Effect of differential thermal contraction on fracture toughness of asphalt materials at low temperatures

Kim, K. W.; El Hussein H. M.

Effect of differential thermal contraction on fracture toughness of asphalt materials at low temperatures

NRCC-42792

Kim, K.W.; El Hussein H. M.

January 1995

A version of this document is published in / Une version de ce document se trouve dans:
Proceedings of the Association of Asphalt Paving Technologists, v. 64, pp. 474-495, 1995

Effect of Differential Thermal Contraction on Fracture Toughness of Asphalt Materials at Low Temperatures

Kwang W. Kim[1] and H.M. El Hussein[2]

Introduction

Thermally induced stresses initiate hairline cracks in asphalt concrete as a result of differential thermal contraction (DTC) which is a consequence of the large difference in coefficient of thermal contraction between aggregate and asphalt cement (i.e., gravel=4 - 5 x 10^{-6}/C, and asphalt cement=0.8 - 2.1 x 10^{-4}/°C) (1). These micro-cracks initiate at the interface between the asphalt matrix (asphalt cement -mineral filler mix) and aggregate. Existence of these cracks suggested by the analytical investigation has been verified later through micro-structural analyses. Analysis of acoustic emission data and visualization through a microscope confirmed the occurrence of localized damage when asphalt concrete samples were exposed to low temperatures (2). These hairline cracks were perpendicular to the aggregate and matrix interface of asphalt concrete samples exposed to low temperatures. Initiation of hairline cracks associated with DTC appeared to be an irreversible process resulting in permanent damage (3). Adhesion and consequently, tensile strength and other performance characteristics of asphaltic concrete, were shown to be significantly affected by DTC. Therefore, other properties such as fracture toughness, fatigue life and creep are also expected to be influenced by DTC due to formation of micro-cracks. This study focusses on the effect of DTC associated damage on fracture characteristics.

Hairline cracks not only function as a source of larger cracks, but also provide a path of least resistance along which other cracks may propagate. Therefore, the presence of hairline cracks due to differential thermal contraction can cause asphalt concrete to be more susceptible to major cracking, and thus reduce its fracture toughness.

Since Moavenzadeh (4) suggested adoption of fracture mechanics concepts to investigate asphalt, other researchers launched similar

[1]Assistant Professor, Kangwon National University, Korea (formerly Canadian Government Laboratory Visiting Fellow) Centre for Surface Transportation Technology National Research Council, Canada
[2]Research Officer, Centre for Surface Transportation Technology, National Research Council Canada
The oral presentation was made by Dr. Kim and Dr. El Hussein

studies (5,6,7,8,9,10,11,12,13) in fracture mechanics of asphalt materials and related topics. Some of these studies were dedicated to investigate low temperature response of asphalt cement (14,15,16,17, 18). The developed concepts focused on a single distress type which was later referred to as low temperature associated cracking (19,20, 21,22,23). These are transverse cracks commonly found in cold regions and are not related to traffic loading. However, little attention was paid to the effect of thermal incompatibility of the asphalt mix components on fracture characteristics of asphalt concrete at low temperature. As mentioned earlier, the concept of DTC suggests the potential for localized damage which does not manifest itself immediately on the pavement surface, but certainly may influence the fracture characteristics of asphalt concrete at low temperature. Therefore, evaluating the effect of DTC on asphalt fracture will improve understanding of low temperature associated problems and their impact on the durability of asphalt pavements.

This study investigates the influence of differential thermal contraction on known fracture properties of asphalt concrete. The study hypothesis is that hairline cracks will develop in a mixture subjected to a sufficiently low temperature and that fracture toughness of the mixture will be substantially lowered. The objective of this study was to evaluate fracture toughness of asphalt concrete as affected by exposure to low temperatures. Since DTC is a phenomenon associated with the non-homogeneity of asphalt concrete, a homogeneous material, i.e., asphalt cement alone or to some extent the asphalt matrix, was not expected to experience damage associated with DTC. Therefore, fracture behavior of asphalt cement and asphalt-filler mixture were evaluated and compared with that of asphalt concrete. This paper presents the laboratory test procedures developed for fracture toughness applied to asphalt materials using the quasi-static three-point bending test setup and conducted at various low temperatures using materials common to Ontario, Canada.

Fracture Toughness of Asphalt

Asphalt is a macromolecular organic material which is a low viscosity Newtonian liquid at high temperatures, a viscous material exhibiting shear-dependent viscoelastic behavior at ambient temperature and a brittle solid at low temperature (24). Therefore, this study will assume that asphalt concrete behaves as an elastic body at temperatures below -5C. However, since no standard method has

been developed for fracture analysis of asphalt materials, an effective crack model (ECM) for plain concrete was used to determine the critical stress intensity factor. It is a direct method for laboratory determination of fracture toughness using results of a single-edge notched beam tested in a three-point bending test. It was developed based on the Griffith relation and modified to take into consideration nonlinear behavior within the process zone (Figure 1) of quasi-brittle materials (25,26). The following equations were used to calculate the critical stress intensity factor, K_{IC}, or fracture toughness, under a three-point bending beam test conditions.

$$K_{IC}=1.138\sigma_n\sqrt{\alpha_e}\,F(\alpha_e) \quad (1)$$

where, σ_n is beam nominal flexural strength given by $3SP_{max} / (2BW^2)$, where S, B and W are defined in Figure 1, $\alpha_e = a_e / W$, effective crack length to beam height ratio, and the correction function $F(\alpha_e)$ is given by

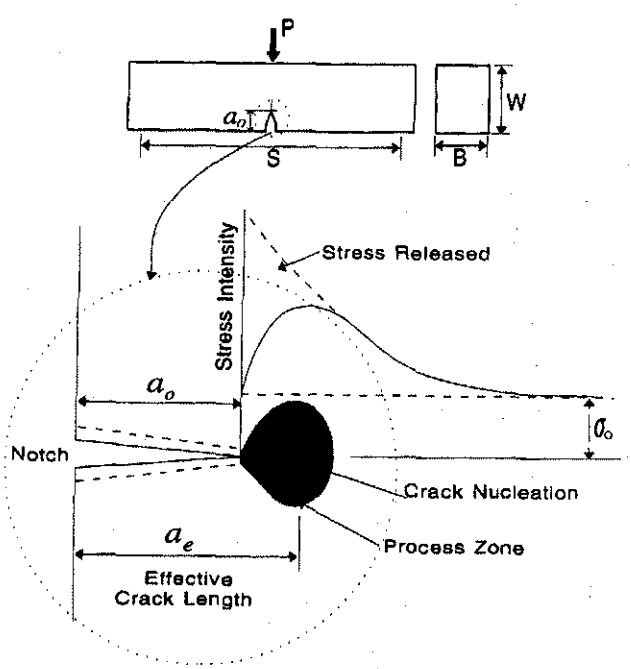

Figure 1 Schematic Illustration of Effective Crack Length, Process Zone and Stress Intensity at Near the Tip of the Notch (after Karihaloo and Nallathambi [26])

$$F(\alpha_e) = \int_0^{\alpha_e} \alpha F^2(\alpha)\, d\alpha \qquad (2)$$

in which, $F(\alpha) = A_0 + A_1 \alpha + A_2 \alpha^2 + A_3 \alpha^3 + A_4 \alpha^4$. The coefficients A_i (i= 0, 1, .., 4) have been given as $A_0 = 0.0075$ S/W + 1.90, $A_1 = -0.08$ S/W - 3.39, $A_2 = -0.2175$ S/W + 15.40, $A_3 = 0.2825$ S/W -26.24, and $A_4 = -0.145$ S/W +26.38, for (S/W) = 4 and 8 with linear interpolation by a RILEM committee (25). The effective crack length, α_e, is the length of the crack that propagated inthe body of the specimen up to peak load (Figure 1). It is assumed that α_e can be calculated by introducing a fictitious beam containing a notch α_e whose stiffness is equivalent to that of the real beam containing a notch depth of α_o , i.e. (16),

$$\delta_{Pmax} = \frac{P_{max}}{4BE}\left(\frac{S}{W}\right)^3\left[1+\frac{5wS}{8P_{max}}+\left(\frac{W}{S}\right)^2\left\{2.70+1.35\frac{wS}{P_{max}}\right\}-0.84\left(\frac{W}{S}\right)^3\right] + \frac{9P_{max}}{2BE}\left(1+\frac{wS}{2P_{max}}\right)\left(\frac{S}{W}\right)^2 F(\alpha_e)$$

in which, δ_{Pmax} and P_{max} are given in Figure 2, and E and w are elastic modulus and weight per unit length of beam, respectively. $F(\alpha_e)$ was given in Equation 2.

For a given notched beam, the initial value of E can be calculated from Equation 3, using $\alpha_o = \alpha_o/W$, multiplying both sides of theEquation by E and dividing both sides of the equation by δ_i after replacing δ_{Pmax} and P_{max} with δ_i and P_i, respectively. Definitions of P_i and δ_i are given in Figure 2. $F(\alpha_o)$ in equation 3 is calculated using Equation 2, and the value of E together with P_{max} and δ_{Pmax} are substituted into Equation 3 to obtain a new value of E, say E_1. The notch depth is increased by $\Delta\alpha = 0.001$ and the procedure repeated until $E_1 = E \pm \epsilon$ (= 0.05 percent) in the trial and error iteration. The value of α at the final step is taken as α_e, and a_e for this value of α_e is considered as an effective crack length.

In these equations P_i and δ_i are used to determine the elastic modulus, E, whereas the P_{max} and δ_{Pmax} are used to estimate the effective Griffith crack length, α_e. The fracture toughness value, K_{IC}, thus calculated using σ_n and α_e is considered essentially independent of specimen size. Linear elastic fracture mechanics formulae are employed after initial notch depth has been suitably augmented to reflect the non-linear load-deflection behavior prior to the attainment

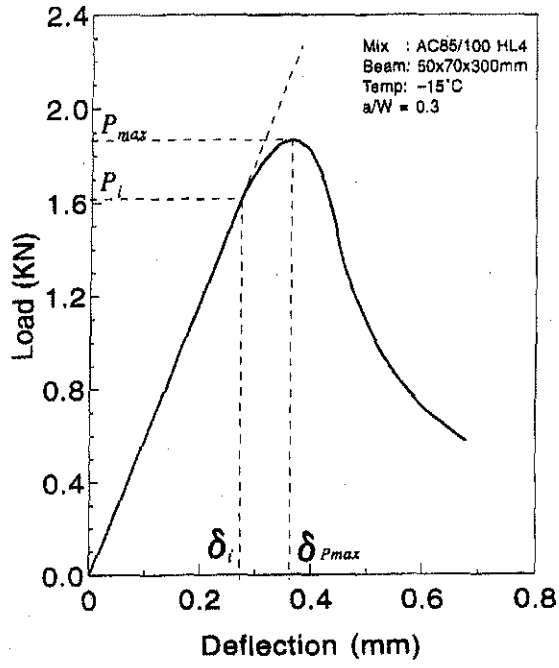

Figure 2 Illustration of a Typical Load and Deflection Curve

of the peak load and no load-deflection information is required past the peak load.

Experimental Program

Materials

An asphalt cement (AC), 85/100 penetration grade, widely used in southern Ontario, Canada, was used as a binder. One mineral filler (limestone dust passing the No. 200 (0.075-mm) sieve) and one aggregate (limestone), with a maximum size of 13.2mm, were used to prepare the aggregate blended shown in Figure 3. Asphalt cement-mineral filler mix, abbreviated here as BF (bitumen-filler), was prepared using asphalt cement and the mineral filler to represent the matrix of a hot dense asphalt mix. A commonly used hot dense asphalt mix referred to as HL4 was designed based on Ontario Ministry of Transportation (MTO) specifications. Physical and mechanical properties of the asphalt concrete mixture are shown in Table 1.

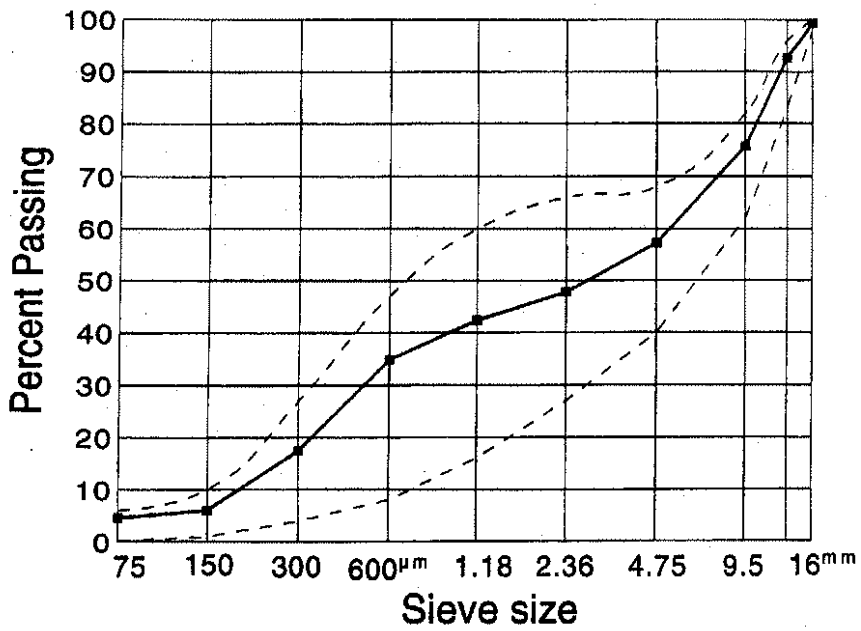

Figure 3 Aggregate Gradation and Specification Limits of HL4 Asphalt Concrete Mix

Table 1. Average Properties of HL4 Asphalt Concrete Mix

Mixture Type	Bulk Specific[1] Gravity	Air Void[2] (%)	Indirect Tensile Strength[3] (KPa)
HL4[4]	2.344	3.8	845.6

[1]determined based on ASTM D2726-90 using saturated surface-dry specimens
[2]calculated based on ASTM D3203-88 using theoretical maximum specific gravity and bulk specific gravity determined using saturated surface-dry specimens
[3]tested at 25C with a loading rate of 50mm/min.
[4]dense hot asphalt mix designed based on MTO specification

Specimens

Beams of asphalt cement (AC), bitumen-filler (BF) and asphalt concrete were made for three-point bending tests. The height (W), width (B) and length of AC and BF beams were 37.5mm, 37.5mm and 160mm, respectively, with a simply supported span S = 150mm, which provides an S/W ratio of 4. The presence of coarse aggregates

in the conventional HL4 mix necessitates the use of a larger beam. The height, width and length of the asphalt concrete beam were 70mm, 50mm and 300mm, respectively, with a span length S = 280mm. An initial notch-depth (a_o) to beam-height (W) ratio (a_o/W) of 0.3 was adopted for all specimens. The depth of the notch was achieved by an insert positioned at the bottom center of the beam mold.

AC beams were prepared by pouring hot-liquid asphalt cement into a metal mold with an insert for the notch in place. Before pouring AC into the mold with the insert in place, a paper soaked in silicon oil was used as a mold lining for easy removal of the cooled specimen. The specimen was conditioned in a cold room at the specified test temperature after removing from the mold. An asphalt content of 18 percent was determined as an optimum content for the BF mix based on earlier trials that accounted for asphalt cement absorbed by coarse aggregate and for the film coating these coarse aggregates. An asphalt content of 5.0 percent was used for the asphalt concrete mix as determined by Marshall mix design. A hand Marshall hammer was used to apply an impact load on the surface of metal plates, one half the beam length and another a full beam length, to compact the hot mixture. There were slight variations in the height of beam due to compaction related factors. The designed compaction provided the mix with approximately the bulk specific gravity achieved on Marshall specimen using 50 blows per side. Three specimens were prepared from each material for each conditioning temperature and the average test results were reported.

Test Procedures

All the beams were loaded using static three-point bending (3PB) test setup to evaluate the material fracture toughness. Asphalt concrete beams were allowed to age for one day at room temperature before storage in the cold room. This period was followed by low temperature conditioning for three days at the specified temperature. Tests were carried out at the same temperature at which beams were conditioned. However, another set of asphalt concrete samples was tested at -5C following the three-day conditioning at various temperatures. For this specific group, the samples were stored at -5C for eight hours prior to loading to make sure that all the beams were tested at approximately the same stiffness.

The number of specimens (beams) assigned for each material and test temperature are shown in Table 2. A computer controlled

hydraulic loading frame and a data acquisition system were used for the test. Two LVDTs were placed at the bottom of the beam, at both sides of the notch, to measure the beam mid span deflection until failure (Figure 4).

Table 2. Experimental Arrangement for Each Material at Specific Temperature

Asphalt Grade	Material Type	Number of Samples at Temperature (C)						
		-35	-30	-25	-20	-15	-10	-5
85/100	Asphalt Cement	0	0	3	3	3	3	3
	Bitumen-Filler	0	3	3	3	3	3	3
	Asphalt Concrete[1]	3	3	3	3	3	3	3
	Asphalt Concrete[2]	0	3	3	3	3	3	3

[1]conditioned and tested at the specified temperature
[2]conditioned at the specified temperature and tested at 5C

Loading rates were selected to provide a 0.1-mm horizontal expansion at the bottom of the beam in one minute. Figure 5 is a schematic diagram illustrating the change in length due to bending of the beam under the action of the load. For a span length of $S = 2r \sin(\theta/2)$, the expanded span length $L = r\theta$, and vertical deflection $\delta = r - r\cos(\theta/2)$. A value of $\theta = 0.09257$ rad was calculated from $S/L = 2\sin(\theta/2)/\theta$ for $S = 280$ and $L = 280.1$. In the same manner, $\theta = 0.12646$ rad was obtained for $S = 150$. Finally, $\delta = 3.24$ and $\delta = 2.40$ were obtained for $S = 280$ and $S = 150$, respectively. Therefore, to achieve the beam expansion rate of 0.1mm/min horizontally, the vertical load was applied to AC and BF beams at a loading rate of 2.4mm/min, and to asphalt concrete beams at 3.24mm/min to account for the difference in length of the two types of beam.

The actual depth of the initial notch, α_o, was measured for each beam after the three-point bending test. Load-deflection profiles at the center of all beams were recorded from the test and later used to calculate fracture toughness, K_{IC}, by substituting in Equations 1 through 3. Elastic modulus, E, was obtained in the course of calculating K_{IC}. Flexural strength, σ_f, was calculated using the beam height minus the initial notch depth, i.e., $\sigma_f = 3SP_{max}/\{2B(W- \alpha_o)\}$.

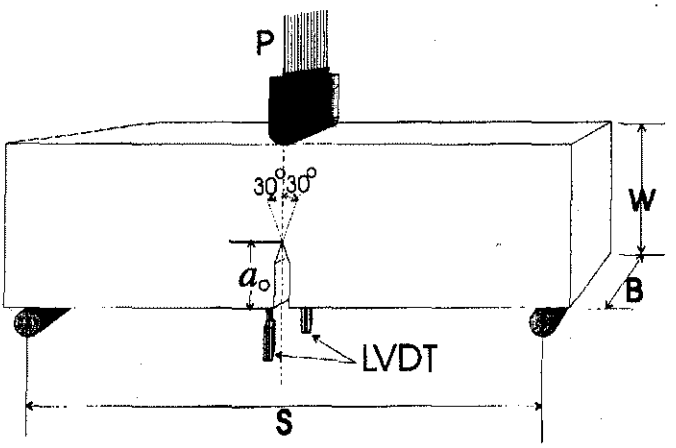

Figure 4 Schematic Diagram of a Notch Beam in a Three-Point Bending Test Setup

Results and Analyses

It is essential to recall details related to differential thermal contraction while interpreting results of the three-point bending test. One important factor is the consideration of asphalt concrete as a composite material where the macrostructure influences the response of the mix to temperature and load induced stresses. A simplifying approximation implemented in the analytical investigation has been adopted here where the bitumen-filler material is considered a uniform material and referred to as the "matrix". It is also important to account for the overall state of stress associated with differential thermal contraction. Considering a simplified geometry where an aggregate particle is surrounded by the asphalt matrix, the tangential tensile stress may cause the localized damage mentioned earlier, however, another stress component must also be accounted for (1). This component is the compressive radial stress which increases the grip of the matrix around aggregate particles prior to the occurrence of the localized damage discussed earlier. The results of such strengthened grip is an improved mechanical adhesion and, therefore, increased resistance to the applied loads.

A typical load-deflection curve at -15C for an asphalt concrete beam is shown in Figure 2. The general shape of the curves for other test temperatures was similar, showing an initial linearity and non-linearity occurring before failure. None of the asphalt concrete beams

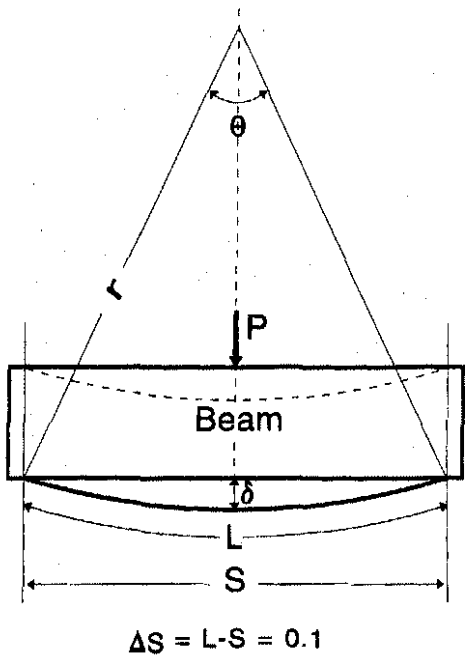

Figure 5 Schematic Diagram Illustrating Bending and Length Change at the Bottom Section of Beam

showed a catastrophic fracture mode during the test. But most of the asphalt cement (AC) and bitumen-filler (BF) beams showed a catastrophic fracture mode. Load and deflection information from three-point bending tests at different temperatures for the three materials are presented in Table 3.

Flexural Strength

Calculated values of the flexural strength based on the results of the three-point bending tests were plotted in Figures 6, 7 and 8 for asphalt cement (AC), bitumen-filler (BF) and asphalt concrete beams, respectively. Considering variation of test results, flexural strength of the pure asphalt (AC) beams shows little change within the investigated temperature range, indicating that the increase in the stiffness of the binder has little effect in this homogeneous material. The flexural strength of the BF (matrix) beams showed a slight drop in flexural strength with temperature drop. The absolute values of the strength were approximately ten times higher than that of asphalt alone. However, asphalt concrete flexural strength (Figure 8)

Table 3. Average Value of Three-Point Bending Test Results for Each Materials

Type of Material	Temp (C)	α_o (mm)	P_i (N)	δ_i (mm)	P_{max} (N)	δ_{Pmax} (mm)
Asphalt Cement	-25	11.36	50.550	0.132	68.000	0.207
	-20	11.19	60.967	0.230	72.000	0.275
	-15	11.12	35.267	0.272	60.433	0.675
	-10	11.17	33.133	0.393	57.533	0.720
	-5	11.17	22.600	0.397	62.300	1.284
Bitumen-Filler	-30	11.75	479.00	0.274	520.00	0.276
	-25	12.22	505.67	0.290	505.67	0.290
	-20	11.12	604.00	0.391	604.00	0.391
	-15	11.16	653.33	0.497	653.33	0.497
	-10	11.18	297.33	0.350	632.67	0.826
	-5	11.15	757.00	0.870	792.00	0.927
Asphalt[1]Concrete	-35	20.23	1022.3	0.137	1337.7	0.203
	-30	20.57	1190.7	0.162	1380.3	0.202
	-25	19.78	1375.3	0.233	1556.7	0.283
	-20	20.35	1430.0	0.203	1653.7	0.252
	-15	20.67	1534.3	0.240	1883.0	0.324
	-10	20.67	1459.3	0.319	1827.7	0.422
	-5	20.22	1096.3	0.229	1687.0	0.433
Asphalt[2] Concrete	-30	21.43	830.3	0.114	1278.7	0.332
	-25	20.97	1022.3	0.111	1660.0	0.265
	-20	20.65	1119.3	0.118	1705.3	0.271
	-15	20.80	1033.0	0.139	1671.7	0.424
	-10	20.79	1162.3	0.138	1671.3	0.324
	-5	20.22	1096.3	0.229	1687.0	0.433

[1]conditioned and tested at the specified temperature
[2]conditioned at the specified temperature and tested at -5C

indicated a completely different behavior compared with the previous, relatively homogeneous, two materials. The strength increased initially, reaching a peak at -15C followed by an approximately 30 percent reduction in strength at -35C. Such a response for asphalt concrete at low temperature has been reported in the literature for other mechanical tests. It includes indirect tensile strength (27) and restraint shrinkage (21) test results. Previous explanations were limited to the effect of stiffness which increases with the drop in temperature, as confirmed by results from this study shown in Figures 9, 10 and 11 for AC, BF and asphalt concrete, respectively.

However, the DTC contribution to the increase in strength can be readily understood through improved adhesion (mechanical bond) as a consequence of increased compressive radial stress (1). Increased stiffness alone did not result in similar behavior in the case of asphalt and bitumen-filler beams since DTC did not affect the integrity of these homogeneous materials.

Differential thermal contraction can also be used to explain the significant drop in flexural strength after peaking. Tangential tensile stresses exceeding the strength of the matrix causes localized damage which has been reported in a previous study as observed through the microscope, and detected from acoustic emissions data (3). Such faults in the matrix reduce significantly the resistance of asphalt concrete to applied loads. At this stage the behavior of the asphalt concrete mix is controlled by that of the matrix, as indicated by flexural strength values shown in Figures 7 and 8, below -20C.

Fracture Toughness

The majority of explanations used to characterize the influence of differential thermal contraction on flexural strength can also be used to explain fracture toughness (K_{IC}) test results. The calculated values of K_{IC} were plotted in Figures 12, 13 and 14 for asphalt cement (AC), bitumen-filler (BF) and asphalt concrete, respectively. Fracture

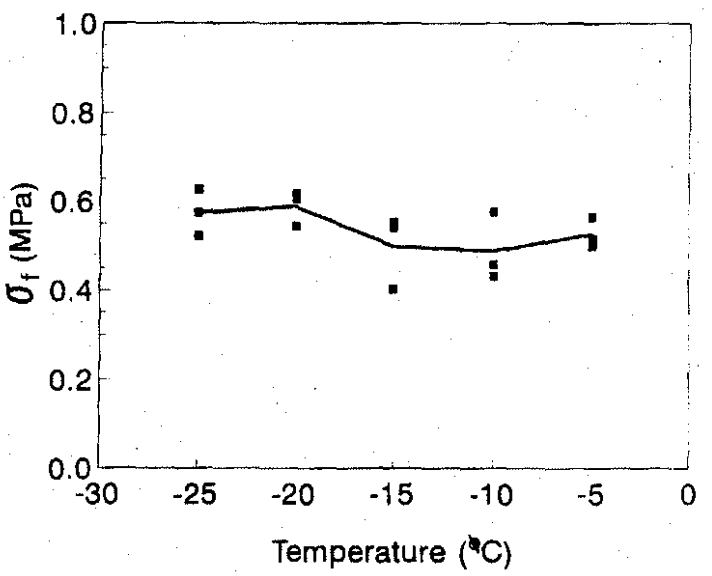

Figure 6 Change of Asphalt Cement Flexural Strength by Temperature

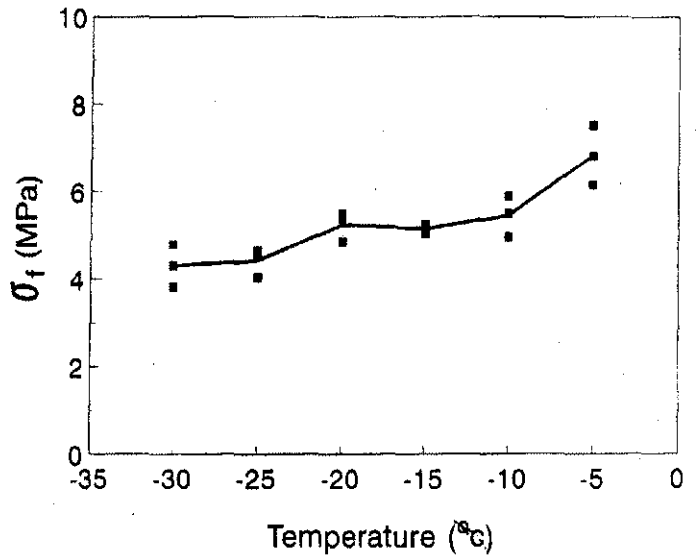

Figure 7 Change of Bitumen-Filler Flexural Strength by Temperature

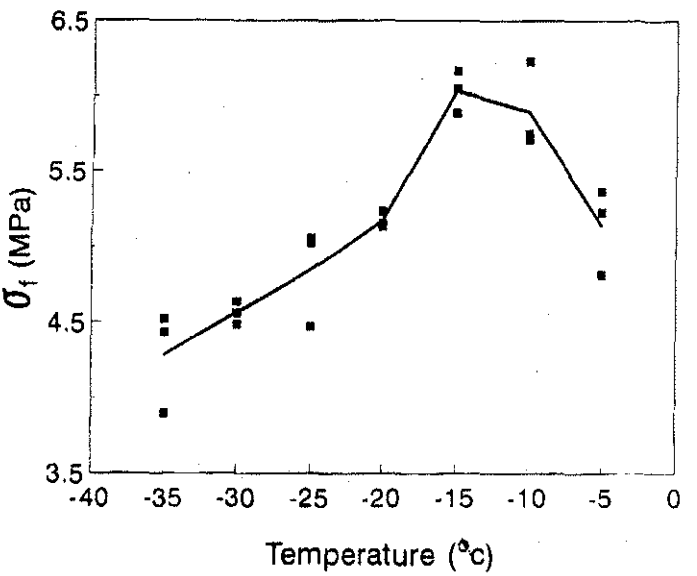

Figure 8 Change of Asphalt Concrete Flextural Strength by Temperature

toughness for AC only showed no sensitivity to temperature drop, indicating that increased stiffness did not result in a reduced K_{IC} value. The fracture toughness in the case of BF (matrix) showed a drop

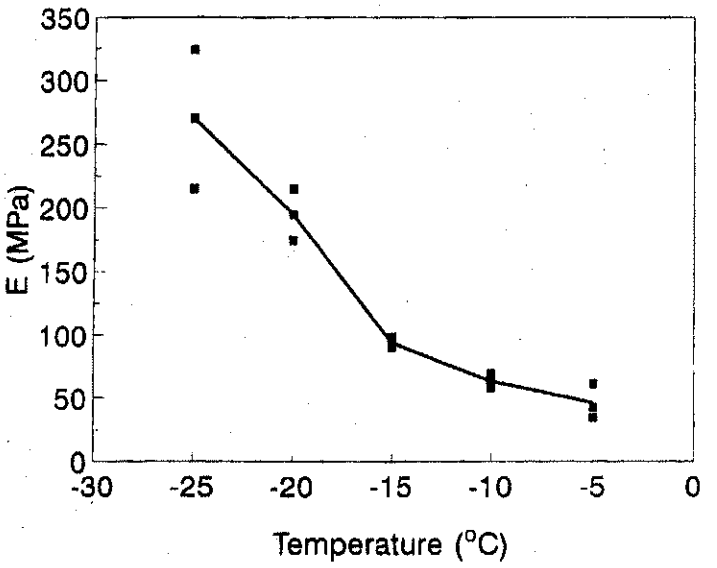

Figure 9 Change of Asphalt Cement Elastic Modulus by Temperature

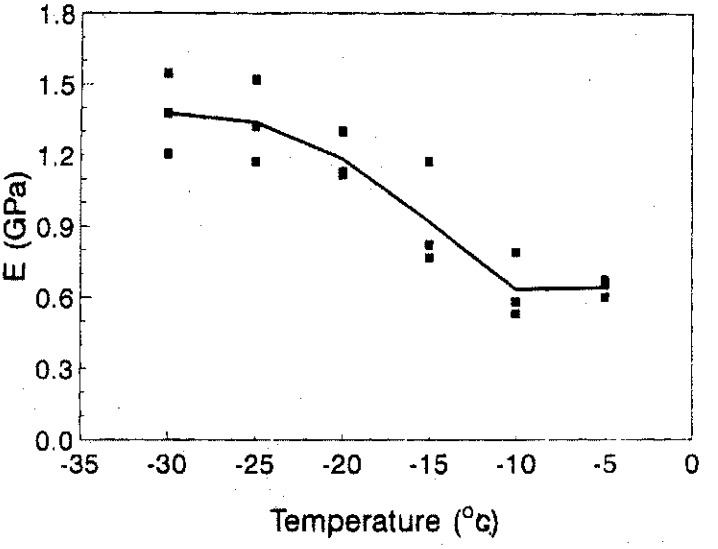

Figure 10 Change of Bitumen-Filler Elastic Modulus by Temperature

which continued up to -30C. However, K_{IC} value for asphalt concrete increased, peaking at -15C, and dropped significantly after that to a value which was slightly higher than that of the matrix. Increased

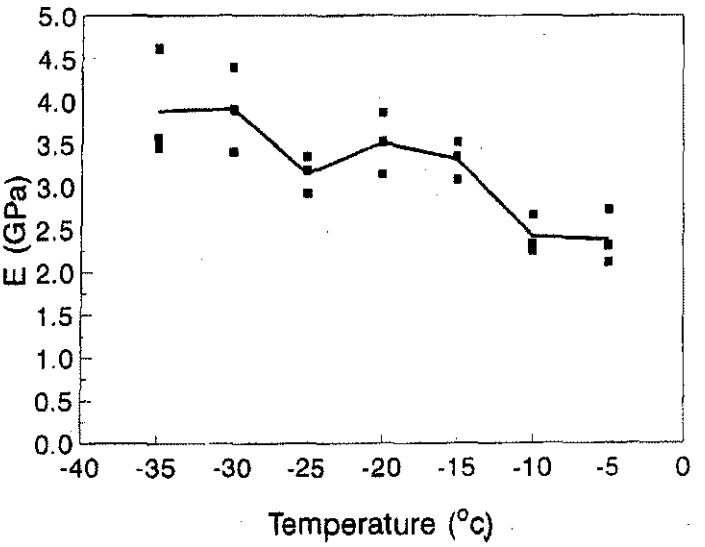

Figure 11 Change of Asphalt Concrete Elastic Modulus by Temperature

mechanical adhesive bond, the result of the compressive radial stress associated with differential thermal contraction, led to the observed increase in fracture toughness.

This situation is demonstrated further by the condition of the failure surface. Figure 15 shows the failure surface of samples categorized by test temperatures. Samples tested above -20C show more broken surfaces of aggregate particles than below -20C. Improved adhesion and the matrix being relatively intact contributed to high fracture toughness above -20C while a weakened matrix resulted in the observed drop in K_{IC} below -20C. Figures 16a and 16b show a close-up of the failure surfaces for two sets of samples tested at two extreme temperatures within the investigated temperature range where the phenomenon of broken aggregate and interface failure is clear. At the relatively high temperature of -5C, a large number of broken aggregates were visible on the failure surface with very little interface fracture showing. But, as a result of a weakened matrix and diminished mechanical bond, for samples tested at -35C, failure occurs close to the aggregate surface (interface) as indicated by the shining surfaces of coated aggregates. Much less broken aggregate is visible compared with samples tested at -5C. As indicated by the fracture toughness temperature relationship for asphalt concrete shown in Figure 14, the propagation of a crack through a weakened matrix must

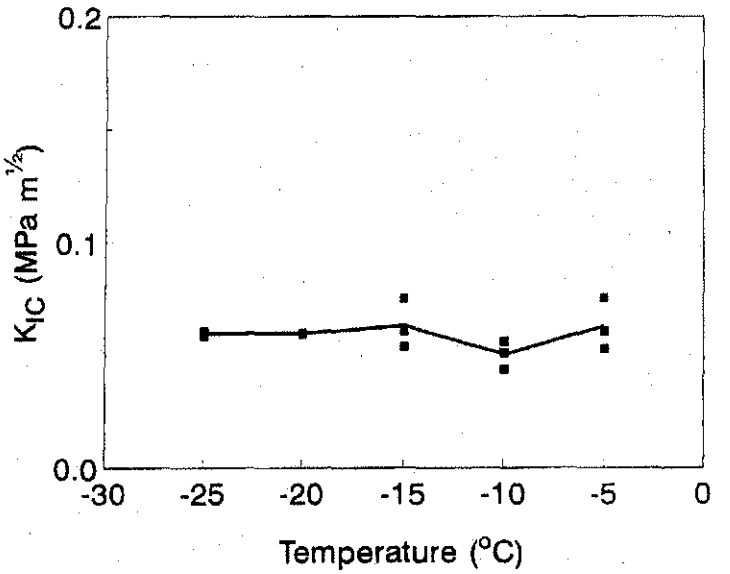

Figure 12 Change of Asphalt Cement Fracture Toughness by Temperature

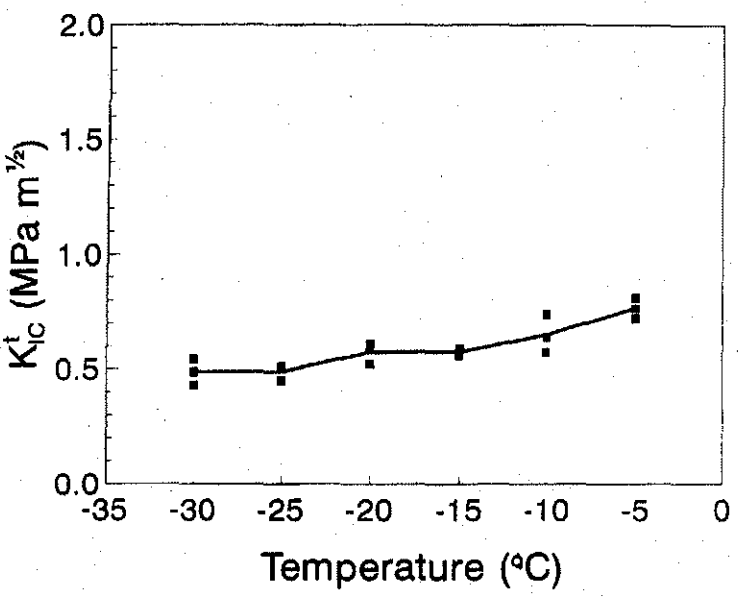

Figure 13 Change of Bitumen-Filler Fracture Toughness by Temperatur

be the reason behind reduced K_{IC} at extremely low temperatures.

It is important to indicate that while flexural strength of asphalt

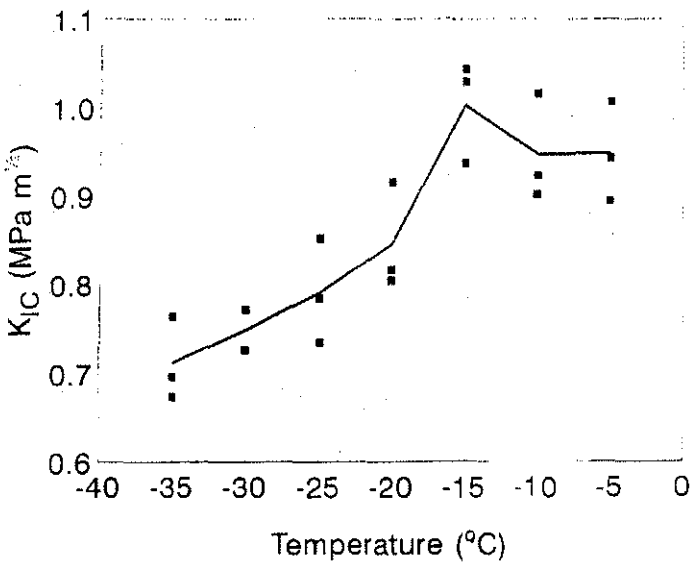

Figure 14 Change of Asphalt Concrete Fracture Toughness by Temperature

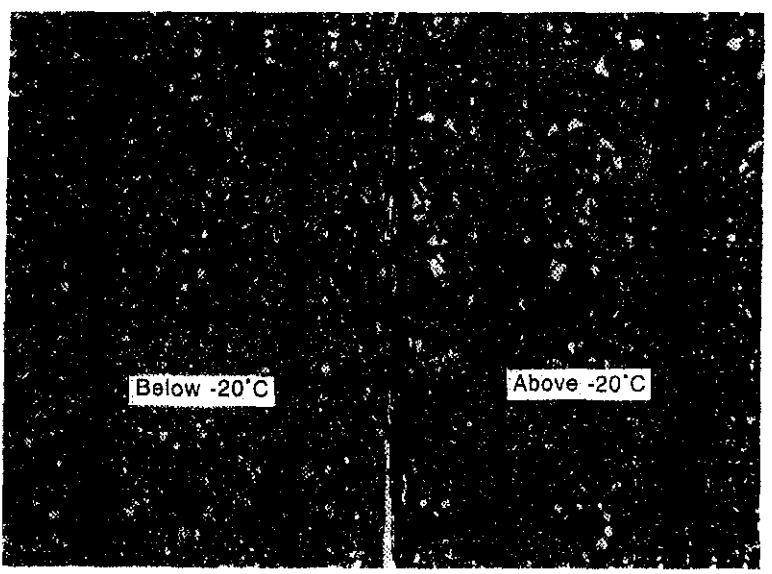

Figure 15 Photograph Illustrating Fracture Faces of Asphalt Concrete Beams Tested Above and Below -20C

concrete dropped to that of the matrix (BF) when localized damage was induced by differential thermal contraction, fracture toughness also decreased but to values higher than that of the matrix. This difference may be explained by the presence of coarse aggregate particles in the crack path which results in the crack traveling longer distance around the particles, leading to K_{IC} values higher than that of the matrix obtained from BF beams. This phenomenon was explained as crack deflection, a type of toughening mechanism which occurred when the path of least resistance was around a relatively strong particle or along a weak interface (28).

In order to investigate whether the induced damage may heal or is of a permanent nature, asphalt concrete beams already conditioned at various low temperatures were stored at a control temperature, -5C, for eight hours and then tested at -5C. The results of this experiment are plotted in Figure 17. For a new mixture exposed to typical low temperatures for the first time, differential thermal contraction seemed to cause the permanent improvement at -10C and -15C. Once the mixture was exposed below these levels of temperature, the damage appeared to be permanent within the studied temperature ranges. Similar improvement occurs following construction when a mix cools down to service temperature.

As mentioned in the analytical investigation, it is not a simple problem to decide whether the final product is an improvement or damage since both mechanisms may occur simultaneously. Locations with sharp aggregate edges will suffer damage at higher temperatures compared with approximately round aggregate particles. Failure at the sharp edges was supported by the results of an earlier microscopic investigation (2). In general, the shape of the curve for fracture toughness, determined at -5C for samples conditioned at various temperatures, is similar to that shown in Figure 14 for samples tested at the conditioning temperature. It seems that improvement and damage were of a permanent nature. Based on these results, it is possible to conclude that localized damage caused by DTC has a significant influence on the fracture behavior of asphalt concrete at low temperatures.

Conclusions and Recommendations

Occurrence of localized damage as a result of tensile stress caused by differential thermal contraction has been supported by existing data and by studies dedicated to investigate this phenomenon. In this

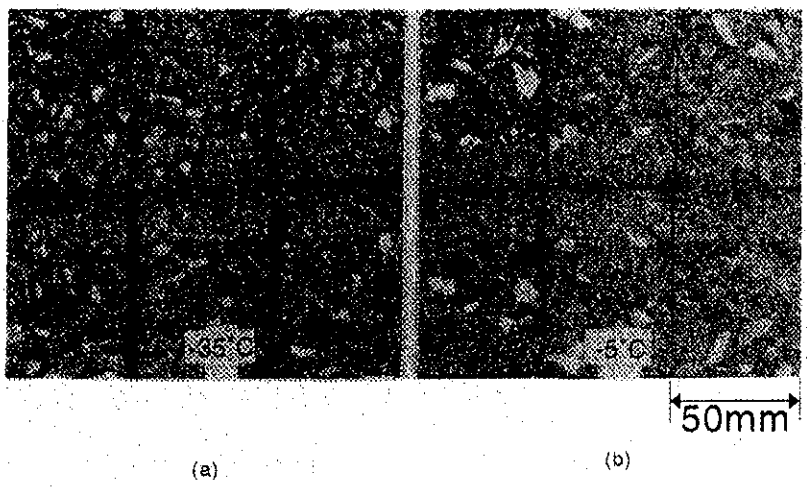

Figure 16 Photograph Illustrating Fracture Faces of Asphalt Concrete Beams Tested (a) at -35C and (b) at -5C

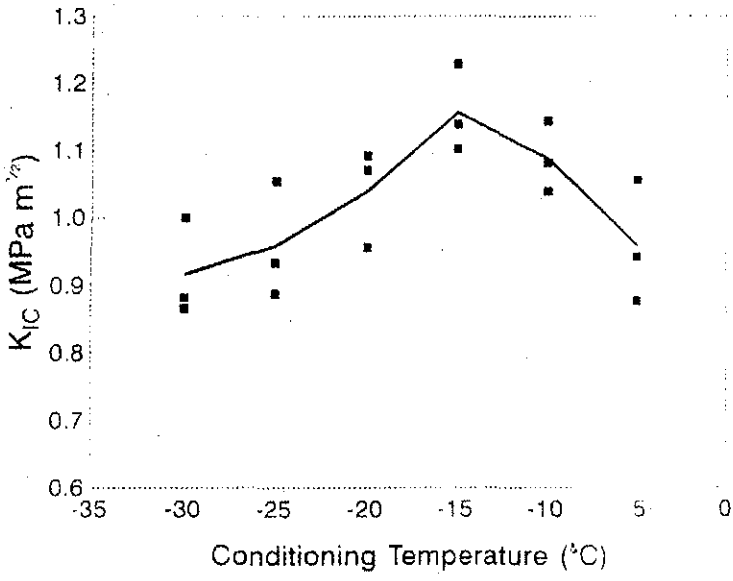

Figure 17 Change of Asphalt Concrete Fracture Toughness by Temperature (Tested at -5C After Conditioning at the Specified Temperatures)

study, the results of three-point bending tests carried out to investigate fracture characteristics of asphalt concrete at low temperatures offered

the following conclusions.

- Exposure of asphalt concrete to extremely low temperatures results in reduced fracture toughness. This reduction can be explained as a direct consequence of hairline cracks caused by differential thermal contraction.
- Two distinct types of failure appeared to result from loading asphalt concrete at various low temperatures. The first type involves crack propagation through the asphalt matrix as well as aggregate, predominantly at above -20C. The second type involves intense interface fracture and limited aggregate breakage indicating the weakened asphalt matrix as a result of damage associated with differential thermal contraction, predominantly appearing below -20C.
- The asphalt matrix properties control the flexural strength and to a lesser extent the fracture toughness of the mix at extremely low temperatures. The presence of aggregate particles along the crack path dictated a longer travel distance and thus a higher fracture toughness for the mix compared with the bitumen-filler mix (matrix).
- Damage associated with low temperature seemed to be of a permanent nature when all samples were evaluated at -5C. However, quantification of the extent of the contribution of DTC associated damage on performance remains difficult because of the complexity of the state of stress.
- Further investigations are required to compare the performance of other mixes using softer asphalts, modified binders and other aggregates with that of the conventional binder mix evaluated in this study.

Acknowledgement

The authors wish to express their appreciation to the Ministry of Transportation of Ontario for partial funding of this research conducted at the Centre for Surface Transportation Technology of National Research Council Canada.

References

1 H.M. El Hussein, and A.O.A. Halim, "Differential Thermal Expansion/ Contraction - A Mechanical Approach to Adhesion in Asphalt Concrete," Canadian Journal of Civil Engineering, Vol. 20, No. 3., 1993, pp. 366-373.

2 "The Effect of Differential Thermal Contraction on Asphalt-Paving Mixture," Interim Report, MTO-R&D Project No. 21270, CSTT/NRC Project No. PJC05, Centre for Surface Transportation Technology, NRC, Ottawa, Canada, 1994.
3 H.M. El Hussein, K.W. Kim, and N.K. Sinha, "Low Temperature Associated Damage Assessment through Microscopic and Acoustic Emission observation," Submitted to Canadian Journal of Civil Engineering, 1994.
4 F. Moavenzadeh, "Asphalt Fracture," Proceedings, AAPT, Vol. 36, 1967, pp. 51-79.
5 H. Aglan, A. Othman, and L. Figueroa, "The Specific Energy of Damage as a Fracture Criterion for Asphalt Pavements," Paper No. 940299, 73rd TRB Annual Meeting, Washington, D.C., 1994.
6 D.A. Anderson, D. Christensen, R. Dongre, M.G. Sharma, J. Runt, and P. Jordhal, "Asphalt Behavior at Low Temperatures," Publication No. FHWA-RD-88-078, FHWA, US Dept. of Transportation, March, 1990.
7 A.G. Bahgat, and M. Herrin, "Brittle Fracture of Asphalt Mixtures," Proceedings, AAPT, Vol. 37, 1968, pp. 32-55.
8 R. Dongre, M.G. Sharma, and D.A. Anderson, "Development of Fracture Criterion for Asphalt Mixes at Low Temperatures," TRR 1228, TRB, 1989, pp. 94-105.
9 L.H. Irwin, "Use of Fracture Energy as A Fatigue Failure Criterion," Proceedings, AAPT, Vol. 46, 1977, pp. 41-63.
10 D.N. Little, and K. Mahbob, "Engineering Properties of First Generation Plasticized Sulfur Binders and Low Temperature Fracture Evaluation of Plasticized Sulfur Paving Mixtures," TRR 1034, TRB, 1985, pp. 103-111.
11 K. Majidzadeh, E.M. Asp, and D.V. Ramsamooj, "Application of Fracture Mechanics in the Analysis of Pavement Fatigue" Proceedings, AAPT, Vol. 40, 1971, pp. 227-245
12 Y.M. Salam, and C.L. Monismith, "Fracture Characteristics of Asphalt Concrete," Proceedings, AAPT, Vol. 41, 1972, pp. 215-256.
13 A.P.S. Selvadurai, P.E. Joseph, and A.O.A. Halim, "Evaluation of Fracture Resistance of Bituminous Materials," Proceedings, Canadian Society for Civil Engineering Annual Conference, Fredericton, N.B, 1993.
14 H.K. Huynh, T.D. Khong, S.L. Malhotra, and L.P. Blanchard, "Effect of Molecular Weight and Composition on the Glass Transition Temperatures of Asphalt," Analytical Chemistry, Vol. 50, No. 7, 1978, PP. 976-979.
15 N.K. Lee, and S.A.M. Hesp, "Low Temperature Fracture Toughness of Polyethylene-Modified Asphalt Binders," Paper No. 940185, 73rd TRB Annual Meeting, Washington, D.C., January 1994.
16 S.C. Leung, and K.O. Anderson, "Evaluation of Asphalt Cements for Low Temperature Performance," TRR 1115, TRB, 1987, pp. 23-32.
17 Y. Wada, and H. Hirose, "Glass Transition Phenomena and Rheological Properties of Petroleum Asphalt," Journal of the Physical Society of Japan, Vol. 15, No. 10, October 1960, pp. 1885-1894
18 L. Zanzotto, P. Siska, D. Foley, and K. Ho, "On Some Low Temperature Characteristics of Conventional and Polymer Asphalts," Proceedings, 35th Annual Conference of Canadian Technical Asphalt Association, 1990,pp.136-158
19 A.A. Abdulshafi, and K. Majidzadeh, "J-Integral and Cyclic Plasticity Approach to Fatigue and Fracture of Asphalt Mixtures," TRR 1034, TRB, 1985, pp. 112-